

Development of mathematical modeling of multi-phase flow of Casson rheological fluid: Theoretical approach



Mubbashar Nazeer^a, Farooq Hussain^b, M.K. Hameed^c, M. Ijaz Khan^d, Fayyaz Ahmad^e, M.Y. Malik^f, Qiu-Hong Shi^{g,*}

^a Department of Mathematics, Institute of Arts and Sciences, Government College University Faisalabad Chiniot Campus, 35400, Pakistan

^b Department of Mathematical Sciences (FBAS) BUITEMS, Quetta 87300, Pakistan

^c Department of Mathematics, Riphah International University Faisalabad Campus, 38000 Pakistan

^d Department of Mathematics and Statistics, Riphah International University I-14, Islamabad 44000, Pakistan

^e Department of Applied Sciences, National Textile University Faisalabad 38000 Pakistan

^f Department of Mathematics, College of Sciences, King Khalid University, Abha, 61413, Kingdom of Saudi Arabia

^g Department of Mathematics, Huzhou University, Huzhou 313000, P. R. China

ARTICLE INFO

Article history:

Received 13 April 2021

Revised 25 May 2021

Accepted 12 June 2021

Keywords:

Casson rheological fluid
Multi-phase flow
Hafnium particles
Exact solution
Gravitational force
Magnetic field

ABSTRACT

Theoretical study of a rheological fluid suspended with two types of nanoparticles through a steep channel is presented in this article. Each suspension is formed by using the non-Newtonian Casson fluid model as the base liquid. Particulate flows are generated mainly due to the effects of gravitational force. In addition to this, the contribution of transversely applied magnetic fields is also considered. Further, the flow dynamics of Casson multiphase flows are compared with the ones suspended with the Newtonian fluid model. A closed-form solution is obtained for the mathematical modeled nonlinear partial differential equations which are transformed into a set of the ordinary differential equation. Separate expressions for volumetric flow rate and pressure gradient have been formulated, as well. Numerical results computed in the different tables show that Hafnium particles gain more momentum than crystal particles. Owing to, many engineering applications of highly thick multiphase flows, such as in chemical and textile industries, it is evident that Casson multiphase suspensions are quite suitable for coating purposes. Moreover, magnetized multiphase flows are compared with the previous investigation as the limiting case for the validation.

© 2021 Elsevier Ltd. All rights reserved.

1. Introduction

Most of the natural, geological and industrial flows are the suspension of non-Newtonian fluids. It is not very easy to predict the flow characteristics of non-Newtonian fluids. This appeals to the interests of scientists to explore the rheological properties of such fluids, mainly due to daily application in petroleum, chemical, and textile industries. Some very commonly known fluids that exhibit these properties are Eyring-Powell fluid [1-3], Micropolar fluid [4,5], Tangent-Hyperbolic fluid [6,7], Power-law fluid [8], Maxwell fluid [9], Rabinowitsch fluid [10,11], Jeffrey fluid [12], Couple Stress fluid [13,14]. Fluids with viscoelastic properties attract the attention of researchers. This type of fluids considered as the special type of the non-Newtonian, because the fluid flow takes place only when the applied stress is greater than critical values (is

called yield stress). The rheological fluid models namely, Herschel-Bulkley fluid model [15], Bingham fluid model [16], and Casson fluid model [17] are established to capture the flow behavior of the viscoelastic fluids. The Casson fluid models are commonly used to highlight the shear thinning behavior in the fluids. In recent years, the Casson fluid model is adopted by the food industries, such as to manufacture chocolate and cocoa. Moreover, in biomedical sciences, the Casson fluid model also assists to predict the development of the rheological characteristics of human blood [18,19]. Some other significant applications of Casson fluid models in different fields are laid down in the list of references [20-24].

Multiphase flow is a ubiquitous phenomenon that deals with the simultaneous transportation of more than one phase. However, many mechanical, chemical, and textile flow mechanisms are multiphase. Turkyilmazoglu [25] used the dust particles to investigate the multiphase flow over a rotating disk. He noted that the velocity of dust particles is greater than the velocity of the fluid phase. Nazeer et al. [26-29] used the nano metallic particles of crystal and hafnium to obtain different types of non-Newtonian multiphase

* Corresponding author.

E-mail address: shiqihong@zjhu.edu.cn (Q.-H. Shi).

Nomenclature

V_f	The velocity of the fluid phase
V_p	The velocity of the particle phase
u, v, w	Velocity components
u_p	The velocity of the particle
u_f	The velocity of the fluid
T	Extra stress tensor for Casson fluid
E	Electric field
J	Current vector
B	Magnetic field
S	Drag force
C	Particles Concentration
M	Hartman number
G	Gravitational force
p	Pressure
δ	Wavelength
ϵ	Dielectric permittivity
Λ	Wavelength
μ_s	The viscosity of the fluid
ρ_f	The density of the fluid
ρ_p	Density of particle
l	Distance between plates
α	The inclination of the channel
Fr	Froude's number
∂	Partial differential
$\frac{D}{Dt}$	Material time derivative

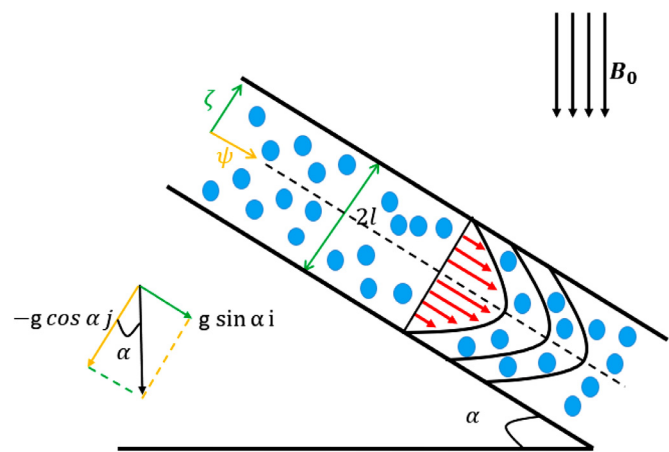


Fig. 1. Flow Geometry.

2. Mathematical modelling

Consider a steady and incompressible flow of a bi-phase non-Newtonian Casson fluid mixed up with Hafnium and crystal metal nanoparticles flowing in a steep channel having some inclination. Let $\mathbf{V}_f = [u_f(x, y), 0, 0]$ and $\mathbf{V}_p = [u_p(x, y), 0, 0]$ are indicating the velocity profiles of fluidic and particulate phases, respectively. The sketch of the under consideration channel is shown in Fig. 1. The occurring equations are solved in two separate sections for fluid and particle phases.

2.1. Fluid phase

The equation of continuity and mass of fluid phase are defined by [26-28].

$$\nabla \cdot \mathbf{V}_f = 0. \quad (1)$$

$$\rho_f(1-C) \frac{D V_f}{D t} = -(1-C) \nabla \cdot p + (1-C) \nabla \cdot \tau_{ab} - SC(V_p - V_f) + J \times B + g \rho_f. \quad (2)$$

The electromagnetic force in above is defined as

$$\mathbf{J} = \sigma(E + V_f \times B), \quad (3)$$

Neglecting the contribution of applied electric field and considering the contribution of transverse and uniform magnetic field, one gets the final

$$E = 0, \quad (4)$$

$$\mathbf{B} = (0, B_0, 0), \quad (5)$$

$$J \times B = -\sigma B_0^2 u_f i. \quad (6)$$

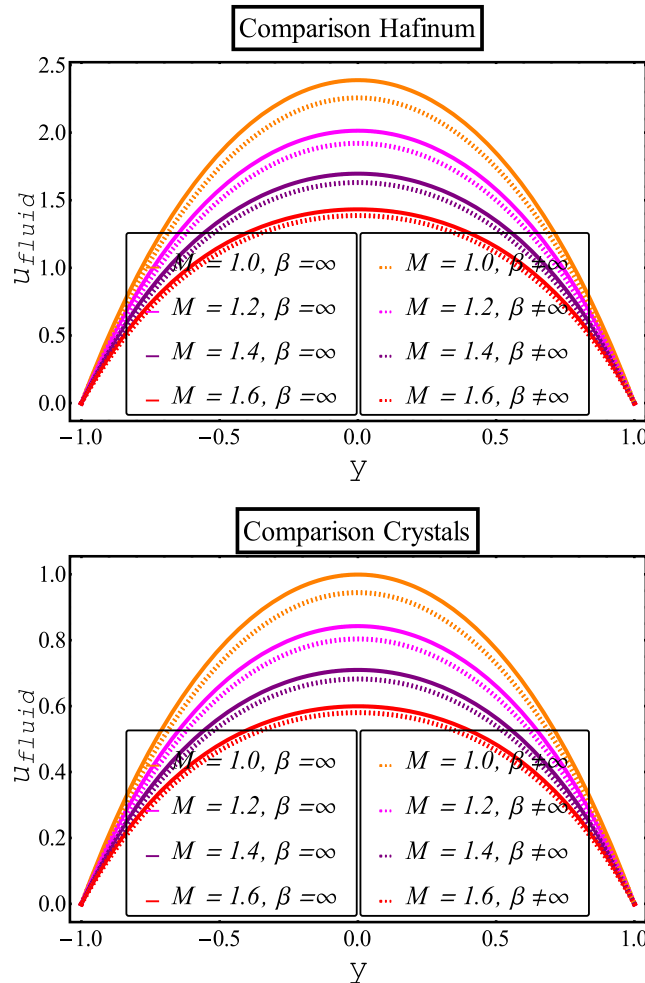
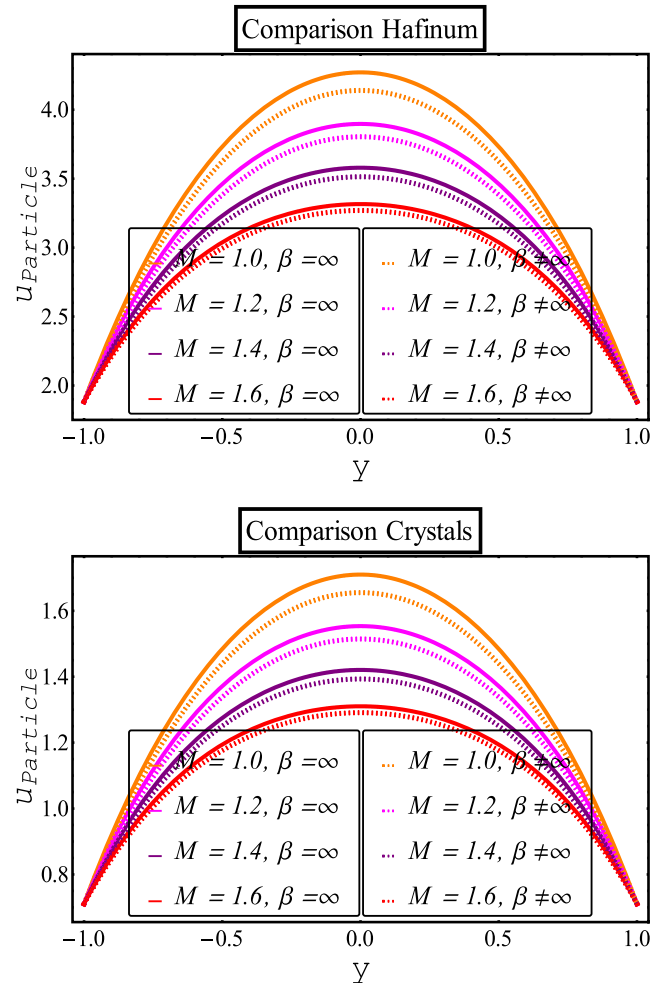
In the last equation " τ_{ab} " is known as the extra stress tensor for Casson fluid such as

$$\tau_{ab} = \begin{cases} 2(\mu_s + p_y/(2\pi)^{1/2})e_{ab}, & \pi > \pi_c \\ 2(\mu_s + p_y/(2\pi)^{1/2})e_{ab}, & \pi < \pi_c \end{cases} \quad (7)$$

2.2. Particle phase

The continuity and momentum equations for the particle phase [29] are expressed as

$$\nabla \cdot \mathbf{V}_p = 0, \quad (8)$$

Fig. 2. Fluid velocity via M .Fig. 3. Particle velocity via M .

$$\rho_p C \frac{D V_p}{D t} = -C \nabla \cdot p + SC(V_p - V_f) + g \rho_p. \quad (9)$$

In components form, Eqs. (1), (2), (8) & (9) are given in the following form,

$$\frac{\partial u_f}{\partial y} = 0. \quad (10)$$

$$\left. \begin{aligned} \rho_f(1-C)\left(\frac{\partial u_f}{\partial t} + u_f \frac{\partial u_f}{\partial x} + v_f \frac{\partial u_f}{\partial y}\right) &= -(1-C) \frac{\partial p}{\partial x} \\ +(1-C)\mu_s(1+\frac{1}{\beta})\left(\frac{\partial^2 u}{\partial y^2}\right) - SC(u_p - u_f) - \sigma B_0^2 u_f + g \rho_f \sin \alpha, \end{aligned} \right\} \quad (11)$$

$$\frac{\partial u_p}{\partial y} = 0. \quad (12)$$

$$\rho_p C \left(\frac{\partial u_p}{\partial t} + u_p \frac{\partial u_p}{\partial x} + v_p \frac{\partial u_p}{\partial y} \right) = -C \frac{\partial p}{\partial x} - SC(u_p - u_f) + g \rho_p \sin \alpha. \quad (13)$$

2.3. Boundary conditions

The above flow problem is analyzed subject to the following boundary conditions:

$$(i) u_f(y) = 0; \text{ When } y = -L, \quad (14)$$

$$(ii) u_f(y) = 0; \text{ When } y = L. \quad (15)$$

3. Homogeneity of the problem

It is essential to take into account the following dimensionless quantities in Eqs. (10)-(15).

$$\left. \begin{aligned} \bar{x} &= \frac{x}{L}, \bar{y} = \frac{y}{L}, \bar{u}_f = \frac{u_f}{u^*}, \bar{u}_p = \frac{u_p}{u^*}, \bar{g} = \frac{g}{g^*}, \bar{\mu}_s = \frac{\mu_s}{\mu_0} \\ F_r &= \frac{u^*}{\sqrt{lg^*}}, \rho_{rel} = \frac{\rho_f}{\rho_p}, \bar{p} = \frac{pL}{u^* \mu_0} M = B_0 L \sqrt{\frac{\sigma}{\mu_0}}. \end{aligned} \right\} \quad (16)$$

Incorporating the above quantities and ignoring the bar signs one finally gets

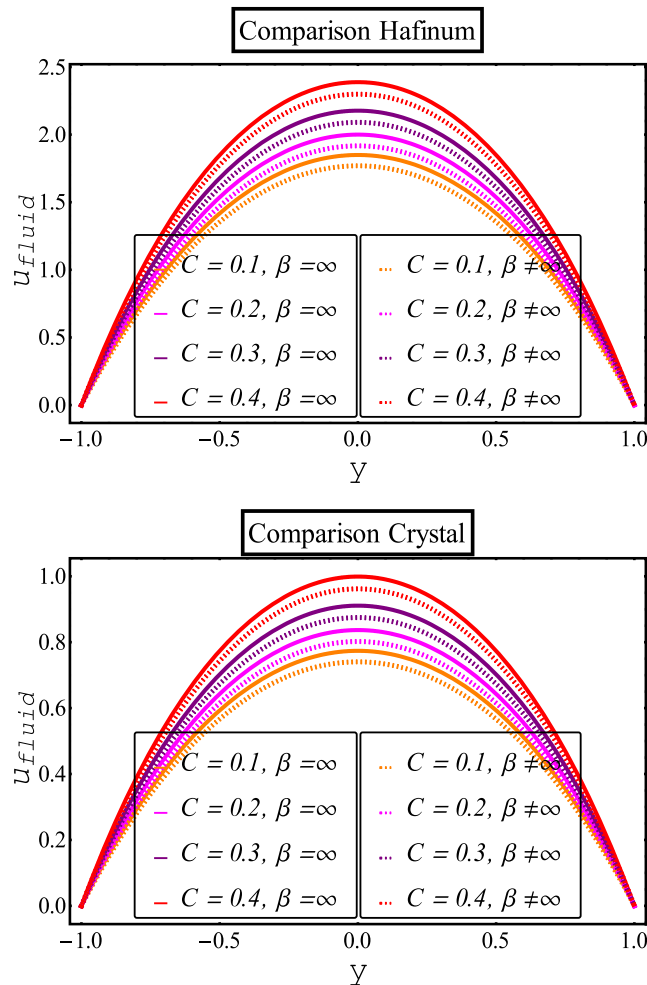
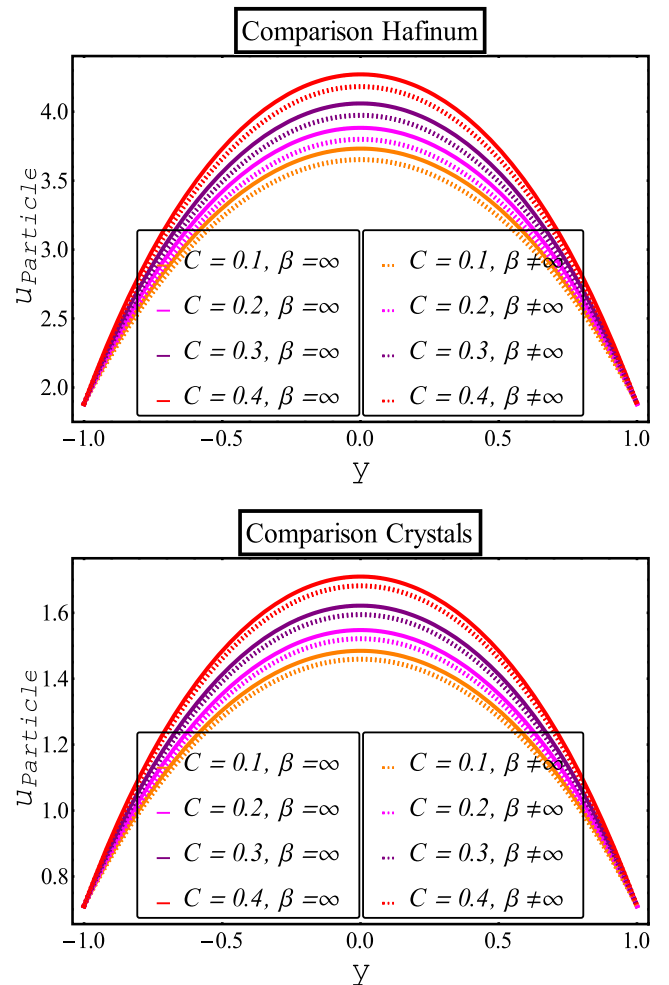
$$\left(1 + \frac{1}{\beta}\right) \frac{\partial^2 u_f}{\partial y^2} - \frac{M^2}{(1-C)} u_f + \left(\frac{n_1 + n_3}{n_1 n_3}\right) \frac{g \sin \alpha}{(1-C)(F_r)^2} - \frac{1}{(1-C)} \frac{\partial p}{\partial x} = 0. \quad (17)$$

$$u_p = u_f - \frac{n_2 n_3 C (F_r)^2 \frac{\partial p}{\partial x} + n_2 g \sin \alpha}{C (F_r)^2 n_3}. \quad (18)$$

Similarly, the corresponding boundary conditions take the form

$$u_f(y) = 0; \text{ When } y = -1. \quad (19)$$

$$u_f(y) = 0; \text{ When } y = 1. \quad (20)$$

Fig. 4. Fluid velocity via C .Fig. 5. Particle velocity via C .

With the assumption of a constant and uniform pressure gradient across the channel, such that

$$\frac{dp}{dx} = P. \quad (21)$$

After some necessary mathematical manipulation Eqs. (17)–(18) become,

$$\frac{\partial^2 u_f}{\partial y^2} - A_1 u_f + A_2 + A_3 P = 0 \quad (22)$$

$$u_p = u_f - \frac{n_2 n_3 C (Fr)^2 P + n_2 g \sin \alpha}{C (Fr)^2 n_3}. \quad (23)$$

One can easily identify in above equations

$$A_1 = \frac{M^2}{(1-C)(1+\frac{1}{\beta})}, \quad A_2 = \left(\frac{n_1 + n_3}{n_1 n_3} \right) \frac{g \sin \alpha}{(1+\frac{1}{\beta})(1-C)(Fr)^2}, \\ A_3 = -\frac{1}{(1+\frac{1}{\beta})(1-C)}. \quad (24)$$

4. Solution of the problem

The momentum of Casson fluid can be obtained by solving Eq. (22) by using the boundary conditions Eqs. (19)–(20). Which

is given as

$$u_f = \left(-\frac{1}{2} \operatorname{Sech} \left[\sqrt{A_1} y \right] A_3 \right) \begin{pmatrix} \cosh \left[\sqrt{A_1} y \right] \\ -\sinh \left[\sqrt{A_1} y \right] \end{pmatrix} \\ + \left(-\frac{1}{2} \operatorname{Sech} \left[\sqrt{A_1} y \right] A_3 \right) \begin{pmatrix} \cosh \left[\sqrt{A_1} y \right] \\ +\sinh \left[\sqrt{A_1} y \right] \end{pmatrix} + A_3, \quad (25)$$

Similarly, the momentum of the particle phase is given as

$$u_p = \left(-\frac{1}{2} \operatorname{Sech} \left[\sqrt{A_1} y \right] A_3 \right) \begin{pmatrix} \cosh \left[\sqrt{A_1} y \right] \\ -\sinh \left[\sqrt{A_1} y \right] \end{pmatrix} \\ + \left(-\frac{1}{2} \operatorname{Sech} \left[\sqrt{A_1} y \right] A_3 \right) \begin{pmatrix} \cosh \left[\sqrt{A_1} y \right] \\ +\sinh \left[\sqrt{A_1} y \right] \end{pmatrix} \\ + A_3 - \frac{C n_2 (n_3 (Fr)^2 P - g \sin [\alpha])}{C n_3 (Fr)^2}. \quad (27)$$

5. Results and discussion

This section narrates the impacts of noteworthy parameters, termed as Hartman number M , particle concentration C , Froude number Fr , Inclination of the channel α , on the flow of both phases, in Figs. 2–9. In each diagram, the dashed lines represent

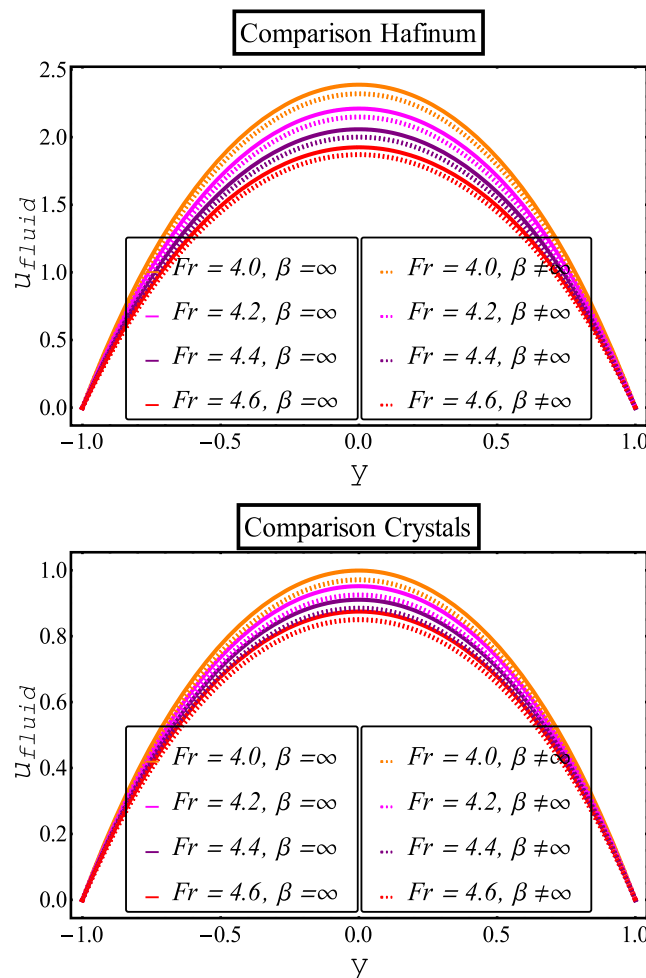


Fig. 6. Fluid velocity via Fr.

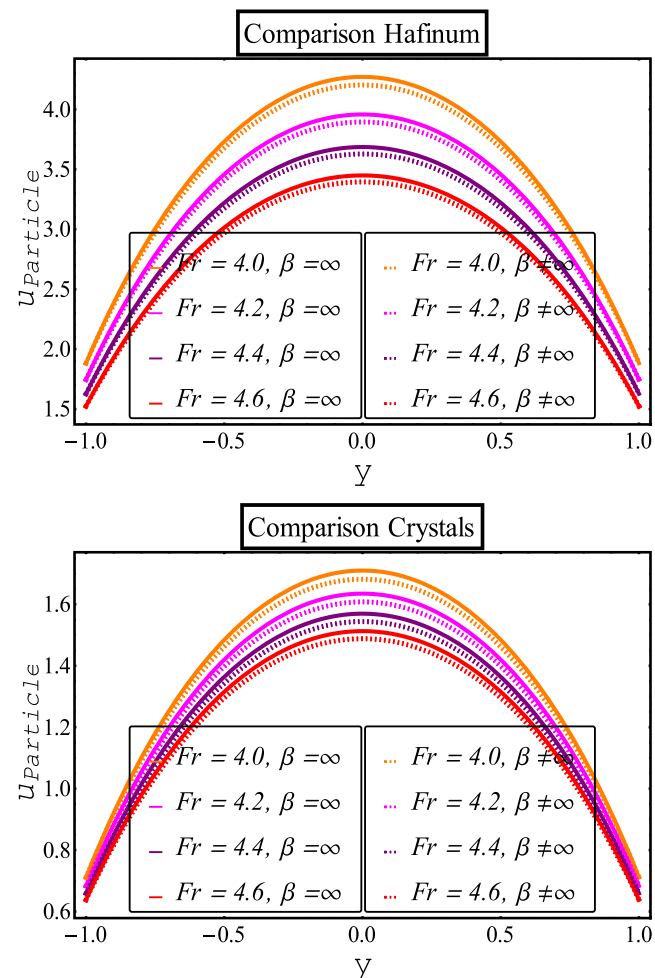


Fig. 7. Particle velocity via Fr.

variation in Casson multiphase flow. While, the solid lines exhibit the variation of the in Newtonian multiphase flow as $\beta \rightarrow \infty$, against the pertinent parameters.

Fig. 2 describes the contribution of the Hartman number on the momentum of the base liquids. It is observed that the velocity of Casson multiphase flows decreases subject to the stronger magnetic fields. Since the application of transverse magnetic fields works as resisting force which retards the motion of the fluid due to Lorentz force. It is to be noted that Newtonian fluid flow through the steep channel is faster than Casson fluid flow. Similarly, multiphase flows which are suspended with Hafnium particles, have greater momentum than the ones which are suspended with crystal particles. Fig. 3 explains the same behavior of each particle against the Hartman number. However, the impact of the magnetic field is greater on crystal particles. The most important quantity for an inclined channel is the Froude number which is a ratio of inertial forces to gravitational force. This dimensionless number is significant to classify the flow. Impacts of Froude number are depicted in Figs. 4–5 on fluid phase and particle phase, respectively. It is witnessed that by enhancing Froude number multiphase flows gradually decreases in Fig. 4. The higher value of the Froude number allows inertial forces to get dominant and hampers the flow motion. The same behavior is for the motion of particle phases in Fig. 5 against the Froude number. In Figs. 6, 7 the comparison graphs for the fluid phase of Newtonian and Casson fluids are drawn for Hafnium and crystal multi-phase flows. The diagrams show a completely different trend in the velocity of the

base liquid. Increasing the number of particles C the momentum of the base fluid increases. Generally, the additional number of particles aggravates the particles' drag force on the main carrier. On the other hand, the effects of gravity undo the application of the drag coefficient. Instead, the mutual collision of the particles further expedites the momentum of the base liquids. The inclination of the slant angle is variated in Figs. 8, 9. By raising the inclination of the steep channel the velocity of the particulate flow rapidly increases. This is according to the physical expectation of the geometry that the higher the inclination, the faster the motion of the multiphase flow.

6. Numerical observations

The present study provides a comparative investigation of Casson two-phase flows and Newtonian two-phase flows, suspended with Hafnium and crystal particles, respectively. The comparative analysis is carried out based on physical properties for the fluid and particle-phase given in Table 1. The velocity of Casson fluid and Newtonian fluid are compared against M , Fr , α , and C , respectively for Hafnium and crystal particles in Tables 2, 3. Multiphase flow suspended with Hafnium particles travels faster than the one suspended with crystal particles for the case of α and C . This is mainly due to the density of the Hafnium metal. On the contrary, an opposite trend has resulted in the case of M and Fr .

Moreover, it is quite eminent from the tabulated numerical data that base fluid's velocity for the case of Newtonian fluid has much greater momentum as compared to Casson fluid. This is indicative

Table 1
Physical properties of given composite flow.

	Density of fluid	Density of particle	Viscosity of suspension	Viscosity of fluid
Base fluid	1200 kgm^{-3}	-	660 pas	125 pas
Hafnium	-	13310 kgm^{-3}	-	-
Crystals	2700 kgm^{-3}	-	-	-

Table 2
Comparison between Newtonian and Casson fluid for the case of fluid phase.

Parameters	u_f (For Hafnium Particles)		u_f (For Crystal Particles)	
	M	C	Newtonian Fluid	Casson Fluid
1.6	0.4	1.43256	1.38626	0.59941
1.4	0.4	1.69638	1.63061	0.70980
1.2	0.4	2.01395	1.92070	0.84269
1.0	0.4	2.38786	2.25675	0.99914
1.0	0.3	2.17696	2.04999	0.91089
1.0	0.2	1.99995	1.87766	0.83683
1.0	0.1	1.84937	1.73189	0.77382

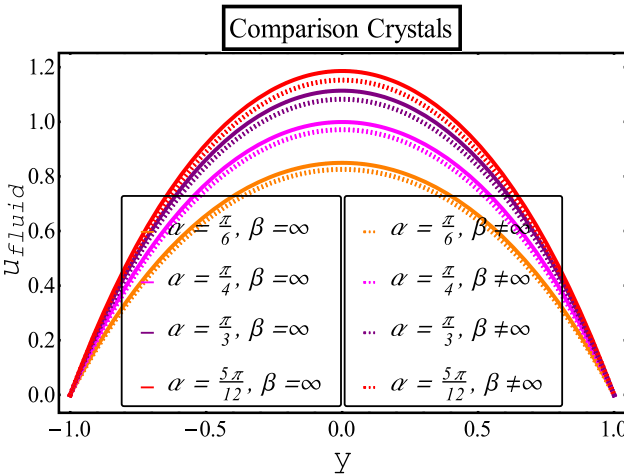
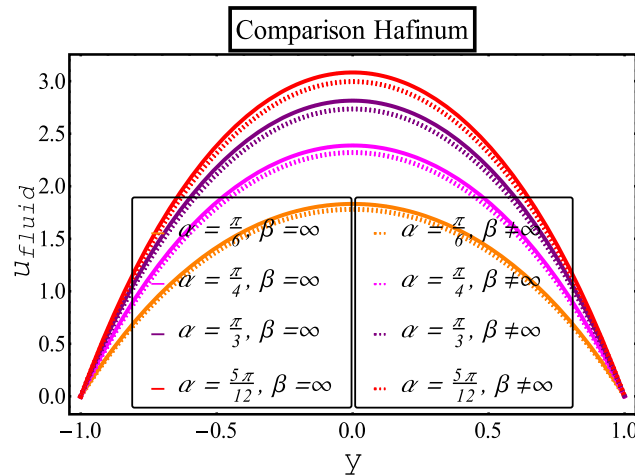


Fig. 8. Fluid velocity via α .

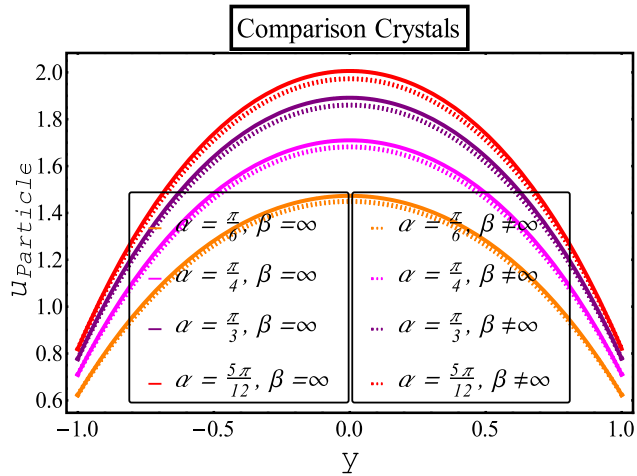
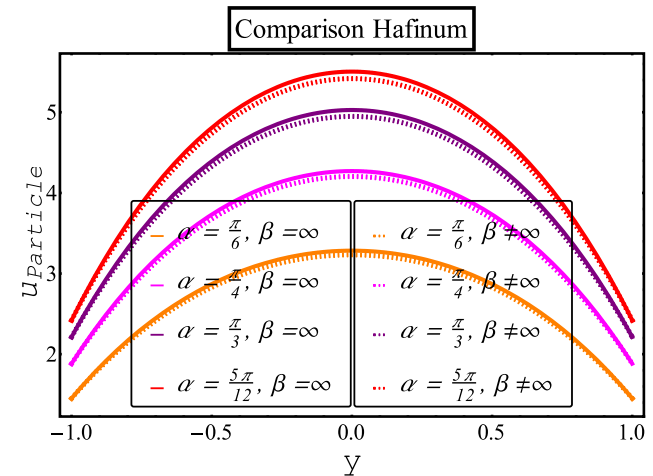


Fig. 9. Particle velocity via α .

that shear stresses and viscous forces are more dominant in Casson multiphase flows.

7. Validation

The current multiphase flows of Casson fluid are compared with existing multiphase flows of a couple stress fluids [39]. Fig. 10 validates the multiphase flows suspended with Hafnium particles and

crystal particles, respectively, for the limiting case i.e. for the Newtonian multiphase flows. Since, current and previous investigations are carried out, through inclined channels. The main source of the flows is gravity while transverse magnetic fields are contributing across the channel. It is to be noted that solid lines (i.e., black and red) represent the solution given by [39]. On the other hand, circular dots describe the current investigation. It is evident from the

Table 3
Comparison between Newtonian and Casson fluid for the case of fluid phase.

Parameters	u_f (For Hafnium Particles)		u_f (For Crystal Particles)		
	Newtonian Fluid	Casson Fluid	Newtonian Fluid	Casson Fluid	
F_r	α				
4.6	$\pi/4$	1.92473	1.81905	0.87465	0.82663
4.4	$\pi/4$	2.05825	1.94523	0.91054	0.86055
4.2	$\pi/4$	2.21129	2.08987	0.95167	0.89942
4.0	$\pi/4$	2.38786	2.25675	0.99913	0.94427
4.0	$\pi/6$	1.83160	1.73103	0.84963	0.80297
4.0	$\pi/3$	2.81469	2.66014	1.11386	1.05270
4.0	$5\pi/12$	3.08301	2.91373	1.18598	1.12086

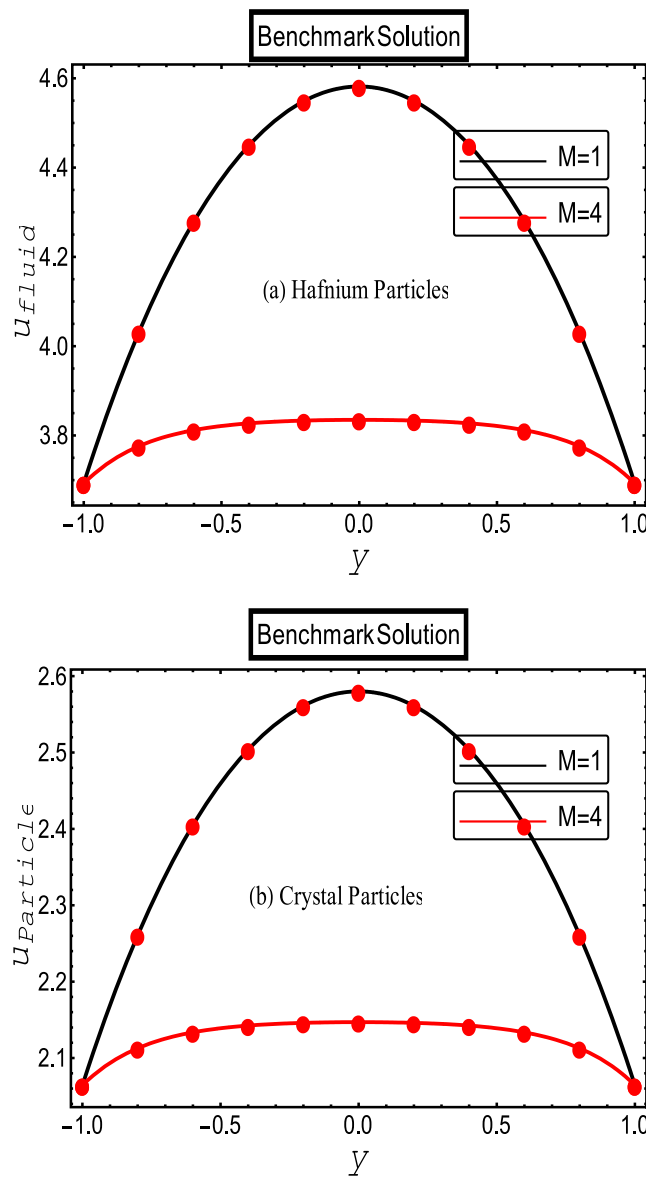


Fig. 10. Comparison between present solution and previous solution.

diagrams that both multiphase solutions are in full agreement as the velocities for Hartman number decreases, gradually.

8. Concluding remarks

Two different types of multi-phase flows are investigated. Comparative analysis is carried out, by taking Casson fluid as the base liquid which suspends with Hafnium and crystal particles, respec-

tively. The main source of the flow is gravitational force through a steep channel. The magnetized multiphase flows, further compared with the existing literature [41] as the limiting case for validation. Some main findings and outcomes of the study are enumerated below:

- Hartman number hampers each type of multiphase flow.
- Casson multiphase flows are more suitable for textile and chemical industries.
- Hafnium suspensions have greater momentum than crystal suspensions.
- Higher the inclination of the channel, the faster the multiphase flow.
- Casson suspension can apply the smooth coating, as compared to Newtonian suspensions.

Credit author statement

All authors agree to publish this manuscript in this journal.

Declaration of Competing Interest

Author has no conflict of interest related to this manuscript.

Acknowledgements

The authors extended their appreciation to the Deanship of Scientific Research at King Khalid University, Abha 61413, Saudi Arabia for funding this work through research groups program under grant number R. G. P-1/75/42.

References

- [1] Turkyilmazoglu M. Eyring-Powell fluid flow through a circular pipe and heat transfer: full solutions. *Int J Numer Methods for Heat and Fluid Flow* 2020;30(11):4765–74.
- [2] Nazeer M. Numerical and perturbation solutions of cross flow of an Eyring-Powell fluid. *SN Appl. Sci.* 2021;3:213.
- [3] Nazeer M, Ahmad F, Saeed M, Saleem A, Naveed S, Akram Z. Numerical solution for flow of an Eyring-Powell fluid in a pipe with prescribed surface temperature. *J. Braz. Soc. Mech. Sci. & Eng.* 2019;41:518–28.
- [4] Turkyilmazoglu M. Flow of a micropolar fluid due to a porous stretching sheet and heat transfer. *Int J Non Linear Mech* 2016;83:59–64.
- [5] Ali N, Nazeer M, Javed T. Finite element simulations of free convection flow inside a porous inclined cavity filled with micropolar fluid. *J Porous Media* 2021;24(2):57–75.
- [6] Nazeer M, Khan MI, Saleem A, Chu Y, Kadry S, Rasheed MT. Perturbation based analytical solutions of non-Newtonian differential equation with heat and mass transportation between horizontal permeable channel. *Numer Methods Partial Differential Eq* 2021:1–24.
- [7] Khan MI, Nazeer M, Shehzad N, Saleem A, Ahmad F. Scrutiny of entropy optimized tangent hyperbolic (non-Newtonian) through perturbation and numerical methods between heated plates. *Adv Mech Eng* 2020;12(12):1–12.
- [8] Shamshuddin MD, Salawu SO, Ogunseye HA, Mabood F. Dissipative power-law fluid flow using spectral quasi linearization method over an exponentially stretchable surface with Hall current and power-law slip velocity. *Int Commun Heat Mass Transfer* 2020;119:104933.
- [9] Sajid M, Abbas Z, Ali N, Javed T. Note on effect of joule heating and MHD in the presence of convective boundary condition for upper-convected Maxwell fluid through wall jet. *J Mol Liq* 2017;230:235–6.

- [10] Chu Y, Nazeer M, Khan MI, Hussain F, Rafi H, Qayyum S, Abdelmalek Z. Combined impacts of heat source/sink, radiative heat flux, temperature dependent thermal conductivity on forced convective Rabinowitsch fluid. *Int. Commun. Heat Mass Transfer* 2021;120:105011.
- [11] Chu Y, Nazeer M, Khan MI, Ali W, Zafar Z, Kadry S, Abdelmalek Zahra. Entropy analysis in the Rabinowitsch fluid model through inclined Wavy Channel: constant and variable properties. *Int. Commun. Heat Mass Transfer* 2020;119:104980.
- [12] Ramesh K, Kumar D, Nazeer M, Waqfi D, Hussain F. Mathematical modeling of MHD Jeffrey nanofluid in a microchannel incorporated with lubrication effects: a Graetz problem. *Phys. Scr.* 2021;96:025225.
- [13] Nazeer M, Hussain F, Iftikhar S, Khan MI, Ramesh K, Shehzad N, Baig A, Kadry S, Chu Y. Mathematical modeling of bio-magnetic fluid bounded within ciliated walls of wavy channel. *Numer Methods Partial Differential Eq* 2021;1–20.
- [14] Nazeer M, Saleem S, Hussain F, Iftikhar S, Al-Qahtani A. Mathematical modeling of bio-magnetic fluid bounded by ciliated walls of wavy channel incorporated with viscous dissipation: discarding mucus from lungs and blood streams. *Int. Commun. Heat Mass Transfer* 2021;124:105274.
- [15] Muravleva L. squeeze flow of Bingham, Casson and Herschel-Bulkley fluids with yield slip at the wall by accelerated augmented Lagrangian method. *J NonNewton Fluid Mech* August 2020;282:104320.
- [16] Fusi L, Farina A. Bingham fluid with viscosity and yield stress depending on the density. *Int J Non Linear Mech* 2020;119:103356.
- [17] KVerma V, Mondal S. A brief review of numerical methods for heat and mass transfer of Casson fluids, *Partial Differential Equations in Applied Mathematics* 2021;3:100034.
- [18] Chakravarty S, Mandal PK. Unsteady flow of a two-layer blood stream past a tapered flexible artery under stenotic conditions. *Computat Methods in Appl Mathem* 2004;4(4):391–409.
- [19] Sankar D, Lee U. Two-fluid casson model for pulsatile blood flow through stenosed arteries: a theoretical model. *Commun. Nonlinear Sci. Numer. Simul.* 2010;15(8):2086–97.
- [20] Aneja M, Chandra A, Sharma S. Natural convection in a partially heated porous cavity to Casson fluid. *Int. Commun. Heat Mass Transfer* 2020;114:104555.
- [21] Ali N, Nazeer M, Javed T, Razzaq M. Finite element analysis of bi-viscosity fluid enclosed in a triangular cavity under thermal and magnetic effects. *Eur. Phys. J. Plus* 2019;134:2.
- [22] Akbar NS. Influence of magnetic field on peristaltic flow of a Casson fluid in an asymmetric channel: application in crude oil refinement. *J Magn Magn Mater* 2015;378:463–8.
- [23] Sulochana C, Payad SS, Sandeep N. Non-Uniform Heat Source or Sink Effect on the Flow of 3D Casson Fluid in the Presence of Soret and Thermal Radiation. *International Journal of Engineering Research in Africa* 2015;20:112–29.
- [24] Samrat SP, Reddy MG, Sandeep N. Buoyancy effect on magnetohydrodynamic radiative flow of Casson fluid with Brownian moment and thermophoresis. *Eur. Phys. J. Spec. Top.* 2021. doi:[10.1140/epjs/s11734-021-00043-x](https://doi.org/10.1140/epjs/s11734-021-00043-x).
- [25] Turkyilmazoglu M. Suspension of dust particles over a stretchable rotating disk and two-phase heat transfer. *Int. J. Multiphase flow* 2020;117:103260.
- [26] Nazeer M, Hussain F, Shahzad Q, Khan IM, Kadry S, Chu MY. Perturbation solution of multiphase flows of Third grade dispersions suspended with Hafnium and crystal particles. *Surf. Interfaces* 2020;22:100803. doi:[10.1016/j.surfin.2020.100803](https://doi.org/10.1016/j.surfin.2020.100803).
- [27] Nazeer M, Hussain F, Shahzad Q, Ali Z, Kadry S, Chu MY. Computational study of solid-liquid supercritical flow of 4th grade fluid through magnetized surface. *Pysica Scripta* 2020;96:015201.
- [28] Nazeer M, Khan MI, Chu Y, Kadry S, Eid MR. Mathematical modeling of multiphase flows of third-grade fluid with lubrication effects through an inclined channel: analytical treatment. *J. Dispers. Sci. Technol.* 2021. doi:[10.1080/01932691.2021.1877557](https://doi.org/10.1080/01932691.2021.1877557).
- [29] Nazeer M, Hussain F, Ahmad O, M SSaeed, Khan MI, Kadry S, Chu Y. Multi-phase flow of Jeffrey Fluid bounded within Magnetized Horizontal Surface. *Surfaces and Interfaces* 2020;22:100846.
- [30] Hussain F, Ellahi R, Zeeshan A. Mathematical Models of Electro-Magnetohydrodynamic Multiphase Flows Synthesis with Nano-Sized Hafnium Particles. *Appl. Sci.* 2018;8:275. doi:[10.3390/app8020275](https://doi.org/10.3390/app8020275).
- [31] Ellahi R, Hussain F, Abbas SA, Sarafraz MM, Goodarzi M, Shadloo MS. Study of Two-Phase Newtonian Nanofluid Flow Hybrid with Hafnium Particles under the Effects of Slip. *Inventions* 2020;5:6. doi:[10.3390/inventions5010006](https://doi.org/10.3390/inventions5010006).
- [32] Firdous H, Husnine SM, Hussain F, Nazeer M. Velocity and thermal slip effects on two-phase flow of MHD Jeffrey fluid with the suspension of tiny metallic particles. *Phys Scr* 2021;96:025803.
- [33] Ge-Jile H, Nazeer M, Hussain F, Khan MI, Saleem A, Siddique I. Two-phase flow of MHD Jeffrey fluid with the suspension of tiny metallic particles incorporated with viscous dissipation and Porous Medium. *Adv Mechan Eng* 2021;13(3):1–15.
- [34] Turkyilmazoglu M. Nanoliquid film flow due to a moving substrate and heat Transfer. *Eur. Phys. J. Plus* 2020;135:781.
- [35] Nazir MW, Javed T, Ali N, Nazeer M. Effects of radiative heat flux and heat generation on magnetohydrodynamics natural convection flow of nanofluid inside a porous triangular cavity with thermal boundary conditions. *Numer Methods Partial Differential Eq* 2021;1–18. doi:[10.1002/num.22768](https://doi.org/10.1002/num.22768).
- [36] Sulochana C, Samrat SP, Sandeep N. Thermal Radiation Effect on MHD Nanofluid Flow over a Stretching Sheet. *Int J Eng Res Africa* 2016;23:89–102.
- [37] Sulochana C, Samrat SP, Sandeep N. Magnetohydrodynamic radiative liquid thin film flow of kerosene based nanofluid with the aligned magnetic field. *Alexandria Eng J* 2018;57(4):3009–17.
- [38] Tili I, Samrat SP, Sandeep N, Nabwey HA. Effect of nanoparticle shape on unsteady liquid film flow of MHD Oldroyd-B ferrofluid. *Ain Shams Eng J* March 2021;12(1):935–94.
- [39] Zeeshan A, Hussain F, Ellahi R, Vafai K. A study of gravitational and magnetic effects on coupled stress bi-phase liquid suspended with crystal and Hafnium particles down in steep channel. *J Mol Liq* 2019;286:110898.